13A.1   ASSIMILATION OF SIMULATED NETWORK RADAR DATA OF VARIED STORM TYPES

USING ENSRF FOR CONVECTIVE STORM ANALYSES AND FORECASTS

Elaine S. Godfrey*, Mingjing Tong, Ming Xue, and Kelvin Droegemeier
School of Meteorology and Center for Analysis and Prediction of Storms
University of Oklahoma, Norman, Oklahoma

1. INTRODUCTION

1.1 *CASA radars*

The National Science Foundation established a new Engineering Research Center for Collaborative Adaptive Sensing of the Atmosphere (CASA) in September 2003 to develop small, low-cost radars for high-resolution sensing of the lower atmosphere.

National Weather Service WSR-88D Doppler radars have limited sampling capabilities in the lower troposphere due to the curvature of the Earth. Thus, meteorological conditions in the lower troposphere are grossly under-sampled, inhibiting forecasts and model initialization in the region where storms develop. The high-spatial-density CASA radars will have the potential to save lives and property by detecting the region of the lower atmosphere that often lies below existing operational WSR-88D Doppler radar coverage (i.e., the lowest three kilometers).

To keep installation costs down, the CASA radars will be placed on cell phone towers or other existing infrastructure with large data transmission capabilities. Unlike the existing pre-programmed radar network, the collaborative CASA radars will communicate with one another and adapt their sensing strategies in direct response to the evolving weather and changing end-user needs. These radar data can be incorporated into numerical weather prediction models for more complete data initialization. The real-time model output could then assist forecasters, government entities, emergency managers, and private industry with decision-making.

1.2 *Ensemble Square-Root Kalman Filter*

The ensemble Kalman filter (EnKF) technique for data assimilation was first introduced by Evensen (1994), and has gained popularity in recent years due to its ease of use and relatively low computational requirements. The original EnKF treats observations as random variables and subjects them to additional perturbations (Evensen 1994, 2003; Burgers et al. 1998; Houtekamer and Mitchell 1998, 2001) such that the analysis error covariance is consistent with that of the traditional Kalman filter (Xue et al. 2005a, hereafter XTD05a). Whitaker and Hamill (2002) developed the ensemble square root Kalman filter (EnSRF) to better estimate the analysis variance by avoiding sampling errors associated with the use of perturbed observations.

This study assesses the potential effects of assimilating radar data on storm-scale numerical weather prediction with a set of observation simulation system experiments (OSSEs). The EnSRF assimilates these data into the model's initial conditions (Whitaker and Hamill 2002; XTD05a). XTD05a developed an EnSRF-based system to assimilate radar data.

This project is a continuation of previous studies that have successfully used the EnKF for the assimilation of simulated Doppler radar data for modeled convective storms (Tong and Xue 2005, hereafter TX05; XTD05a; Xue et al. 2005b, hereafter XTD05b). These studies have demonstrated encouraging results in the model state variables (i.e., u, v, w, p, θ, q_v, etc.) for individual supercell storms, even though radars do not directly observe these variables (XTD05b). In TX05, the best results are obtained when both radial velocity and reflectivity data from the radar emulators are assimilated into the model. In that study, the EnKF showed great ability in retrieving the model state variables when using a general purpose compressible model with a multi-class ice microphysics parameterization. TX05 also showed that dynamically consistent background error covariances develop in the system, most notably in the later cycles, even when velocity data and data outside of the precipitation regions are not assimilated. Thus, the authors concluded that such flow-dependent background error covariances play a crucial role in successful data assimilation and retrieval (XTD05b).

2. ARPS MODEL AND TRUTH SIMULATION

This study is a continuation of earlier work (TX05; XTD05a; XTD05b), which employed an OSSE framework based on the EnSRF to evaluate the impact of data from the CASA and WSR-88D networks on single-thunderstorm forecasts in a nonhydrostatic weather prediction model. Unlike previous studies that were limited to a single idealized supercell case, a multi-cellular convective system is simulated within the radar network. Assimilations and forecasts are performed by incorporating the simulated radar data into the Advanced Regional Prediction System (ARPS) model (Xue et al. 2000, 2001, 2003) using the EnSRF method. The ARPS model is a fully compressible and nonhydrostatic atmospheric prediction system that contains 12 prognostic state variables, including wind components u, v, w, potential temperature θ, pressure p, the mixing ratios for water vapor

Corresponding author address: Elaine S. Godfrey, University of Oklahoma, School of Meteorology, 100 East Boyd Street, Suite 1310, Norman, Oklahoma 73019; e-mail: esavageau@ou.edu.

q_v, snow q_s, and hail q_h, plus the turbulence kinetic energy used by the 1.5-order subgrid-scale turbulence closure scheme (XTD05a). The three-category ice scheme of Lin et al. (1983) parameterizes the microphysical processes.

The horizontal domain size is 180 km × 96 km × 20 km in the x, y, and z directions, respectively, with a horizontal grid spacing of 1.0 km. To better resolve the lower atmosphere, the 40-layer vertical grid is stretched with a minimum vertical resolution of 200 m at the surface. The numerical simulations are initiated in a horizontally homogeneous atmosphere containing an axially symmetric thermal perturbation of horizontal radius 10 km and vertical radius 1500 m. The temperature is increased 4°C at the center (located 1400 m AGL) and decreases gradually to its edge. The bubble is initially centered on the point $x = 30$ km, $y = 70$ km. The origin of the coordinate system is in the southwest corner of the grid. The initial location of the bubble is chosen so that over most of the assimilation period, most of the multi-cellular storm system remains within the domain.

To generate a multi-cellular convective system, the vertical temperature, moisture, and wind-speed profile developed by Weisman and Klemp (1982, hereafter WK82) provided the initially horizontally homogeneous atmosphere in the ARPS model. The environmental potential temperature $\overline{\theta}$ and relative humidity H are given by

$$\overline{\theta} = \begin{cases} \theta_0 + (\theta_{tr} - \theta_0)\left(\dfrac{z}{z_{tr}}\right)^{\frac{5}{4}} & , \quad z \leq z_{tr} \\ \theta_{tr} \exp\left[\dfrac{g}{c_p T_{tr}}(z - z_{tr})\right] & , \quad z > z_{tr} \end{cases} \quad (1)$$

$$H(z) = \begin{cases} 1 - \dfrac{3}{4}\left(\dfrac{z}{z_{tr}}\right)^{\frac{5}{4}} & , \quad z \leq z_{tr} \\ 0.25 & , \quad z > z_{tr} \end{cases} \quad (2)$$

where $z_{tr} = 12$ km, $\theta_{tr} = 343$ K, and $T_{tr} = 213$ K represent the height, potential temperature and actual temperature, respectively, at the tropopause, and $\theta_0 = 300$ K is the surface potential temperature (WK82). The mixing ratio is kept constant at a maximum value $q_{v0} = 18$ g kg^{-1} near the surface to approximate a well-mixed, moist boundary layer conducive to multi-cellular storm development. For a skew-T diagram of a sounding similar to this one, please see WK82. WK82 also developed the wind profile used here, and is given by

$$U = U_s \tanh\left(\frac{z}{z_s}\right), \quad (3)$$

where $z_s = 3$ km and $U_s = 12$ m s^{-1} (after Richardson 1999). A unidirectional shear profile in the x-direction is used for simplicity and because it allows for the application of a symmetric condition of the model equations in
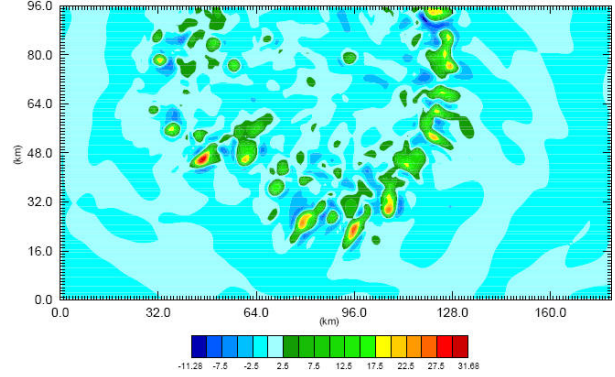

FIG. 1. Horizontal cross section of vertical velocity (m s^{-1}) at 3 hours at $z = 4.6$ km for $U_s = 12$ m s^{-1} and $q_v = 18$ g kg^{-1}.

order to reduce the model domain by one half in future runs. More details on the truth simulation initialization parameters are shown in Table 1.

Storms are allowed to evolve through three hours, using a four-second time step, and grow into a large multi-cellular thunderstorm complex with several strong vertical updrafts (Figure 1). Model conditions are written every five minutes to allow for five-minute volume scan simulations by the radar emulators. Although the system begins as a single vertical updraft, more cells quickly develop as the system grows and spreads eastward and southward, filling most of the domain.

3. RADAR EMULATOR

One existing WSR-88D radar in central Oklahoma (KTLX) and up to four CASA test-bed radars being installed in central Oklahoma are used in this study. As in previous studies (e.g., XTD05a), standard precipitation-mode parameters are assumed. The WSR-88D radar has a 10 cm wavelength, a 1° beam width, a total of 14 elevations with the lowest elevation at 0.5° and highest at 19.5°, and a radial resolution of 250 m for radial velocity and 1 km for reflectivity. The maximum range is assumed to be 230 km, which is sufficient to cover the entire domain. The four radars in the first CASA test-bed will have a three centimeter wavelength (X-band), a 2° beam width, and a maximum range of 30 km. Consistent with the data expected from the CASA network, only data below three kilometers will be used. As in previous studies, a volume scan will consist of ten elevation scans 2° apart, beginning at 1° elevation. Future studies will examine the impact of distributed collaborative adaptive sensing (DCAS) scanning strategies on numerical weather prediction. The initial CASA radars in the Oklahoma test-bed are scheduled for installation in the first few months of 2006 near Chickasha, Rush Springs, Lawton, and Cyril in southwestern Oklahoma. These radars will be about 90 km to the southwest of KTLX, and are shown in Figure 2 with their expected 30 km range rings.

For data sampling and assimilation, the prediction

TABLE 1. List of parameter settings for ARPS model simulations.

Parameters	Value
Horizontal grid spacing (array size)	2 km (75 × 48 points)
Vertical grid stretching function	Hyperbolic tangent
Vertical grid spacing (number of levels)	200 m – 800 m (40 levels)
Time step	4 sec
Coriolis and earth curvature effects	Not used
Fourth-order mixing coefficient	1×10^{-3} s^{-1}
Pressure field de-trending	On
Nondimensional divergence damping coefficient	0.05
Rayleigh damping coefficient (applied above 12 km only)	3.33×10^{-3} s^{-1}
Lateral boundary conditions	Radiation (open)
Lateral boundary relaxation coefficient	0.05
Top & bottom boundary conditions	Rigid wall with upper sponge (wave absorbing layer)
Horizontal & vertical advection scheme	4$^{\text{th}}$ order horizontal, 2$^{\text{nd}}$ order vertical with leapfrog time step
Cumulus parameterization	Not used
Grid-scale microphysics	6-category water/ice microphysics of Lin et al. (1983)
Turbulence parameterization	1.5-order TKE closure
Sub-grid scale turbulence	Isotropic
Radiation parameterization	Not used
Land surface and vegetation scheme	Not used
Computational mixing	4$^{\text{th}}$ order in horizontal, 2$^{\text{nd}}$ order in vertical

model (truth simulation) and the observation operators are assumed to be without error, which is a common assumption in radar OSSE studies. As in XTD05a, the emulated radar data are assumed to be on the original radar elevation angles and then interpolated from the radar polar coordinate to the Cartesian coordinate system. Future work may include studying the effects of such horizontal interpolation by comparing it with data in radar coordinates. Since the emulated radar observations are not yet at the model grid points, a forward observation operator is used to adjust the data from the model's vertical levels to the elevation levels that would be seen by a radar

FIG. 2. Four-radar network for initial CASA deployment and the location of KTLX in Oklahoma. Circles denote the anticipated 30-km radar range.

on the surface. The radar emulator performs power-gain-based sampling in the vertical direction using

$$\varphi_e = \frac{\Sigma G \varphi_g \Delta z}{\Sigma G \Delta z}, \tag{4}$$

where φ_e and φ_g are the elevation level, e, and grid point values, g, of either radial velocity or reflectivity, and Δz is the depth of the layer in which φ_g resides. The power gain function, G, is assumed to be Gaussian and has the form

$$G = \exp\left[-4 \ln 4 \left(\frac{\phi_g - \phi_0}{\phi_w} \right)^2 \right], \tag{5}$$

following Wood and Brown (1997), where ϕ_w is the beam width, ϕ_g is the elevation angle for the grid point value, and ϕ_w is the elevation angle at the beam center.

For radial velocity, the grid point values involved in the numerator of Equation (4) are first calculated from

$$V_{rg} = u \cos\alpha \sin\beta + v \cos\alpha \cos\beta + w \sin\alpha, \tag{6}$$

where α is the local elevation angle and β is the azimuth angle of the radar beam that goes through the given grid point, and u, v, and w are the model velocities interpolated to the scalar point of a staggered model grid. Subscript g denotes the grid point value. Hydrometeor sedimentation effects are not involved in the data or assimilation because the radial velocity is sampled directly from the velocity fields.

Simulated reflectivity, Z (dBZ), is calculated from rainwater, snow and hail hydrometeor mixing ratios with the same formulations as in TX05, XTD05a, and XTD05b and is formally given by
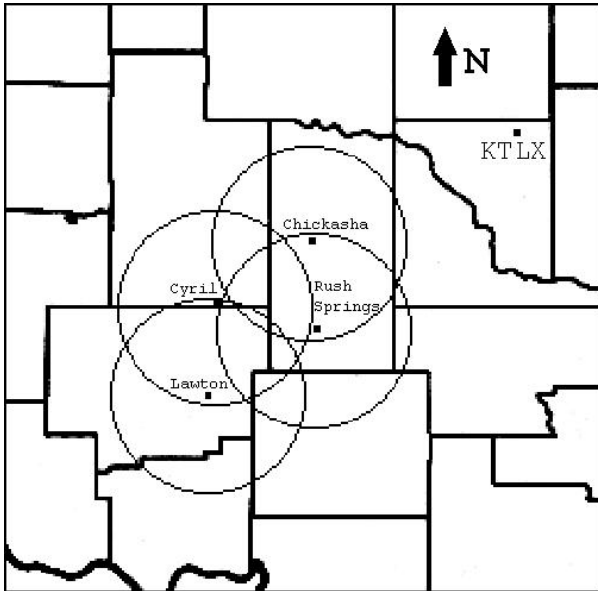
$$Z = Z(q_r, q_s, q_h), \qquad (7)$$

where, following Smith et al. (1975), q_r, q_s, and q_h are rain, snow, and hail mixing ratios, respectively. These formulations are consistent with the Lin et al. (1983) ice microphysics scheme used in the ARPS model. Future work may include studying the effects of attenuation, which may have a significant effect on the CASA radar data.

After the radial velocity and reflectivity are sampled from the grid points, observation errors are simulated by adding Gaussian random errors with zero mean and a standard deviation of 1 m s^{-1} and 5 dBZ for velocity and reflectivity, respectively. It should be noted that no data are collected or assimilated where no grid level lies within the beam width, which is infrequent and serves to naturally thin the data at well-sampled low levels.

4. DATA ASSIMILATION PROCEDURE

Similar to that described in XTD05a and XTD05b, the EnSRF system used here contains 40 ensemble members. For a thorough description, see XTD05a. The initial ensemble forecast will begin at 20 minutes after the model is initialized, allowing for a 100 minute assimilation period and a one-hour forecast. Random perturbations, drawn from a Gaussian distribution with zero mean, will have standard deviations of 3 m s^{-1} for u, v, and w, 3 K for θ, and 0.5 g kg^{-1} for q_v, the mixing ratio for water vapor. These random perturbations will be added to a horizontally homogeneous ensemble mean, defined by the WK82 sounding, to initialize the ensemble except at the lowest grid level above ground and in the outermost five grid points along the lateral boundaries. The radar observations will be assimilated every five minutes in order to simulate the traditional WSR-88D volume scan period, and the first analysis will be performed at 25 minutes. The effective cutoff radius will be determined through numerical experimentation, but is likely to be near 6 km.

Similar to XTD05a and XTD05b, a covariance inflation procedure will be necessary due to the frequent underestimation of the background error covariance that is a result of the limited size of the ensemble. Although based on that of Anderson (2001), this seven percent inflation will only be applied at the grid points where the observations with $Z > 10$ dBZ are of direct influence, instead of being applied to the entire domain. Otherwise, spurious convection would be a significant problem outside regions of precipitation.

5. DISCUSSION

To assess the impact of assimilating CASA radar data from multi-cellular convective systems, several different case studies will be conducted. All of these will involve the truth simulation in the domain described above. The first of these cases will involve ingesting only the data

from the KTLX WSR-88D radar, located just outside the northeast domain corner, such that the CASA network would be centered in the domain. The second case will involve the same placement of the storm and domain, but data from both KTLX and the four CASA radars will be ingested. The third of these cases will ingest only the CASA radar data, and the fourth will look at the effects of assimilating KTLX data and only one well-positioned CASA radar.

If time permits, more dual-network cases will be run with the CASA radars located over either the left or the right portion of the domain, thus comparing the effects of the CASA data on limited portions of the model, while having continual coverage of the upper atmospheric levels by the KTLX radar.

In order to assist the development of DCAS strategies for the first CASA network and to assess the potential effects of these strategies on storm-scale numerical weather prediction, further OSSEs will be conducted with the ARPS model for additional convective storm types. For each of these storm types, the importance of temporal sampling, forecast sensitivity, areal coverage of the radars, and clear-air sampling in DCAS will be evaluated.

REFERENCES

Anderson, J. L., 2001: An ensemble adjustment Kalman filter for data assimilation. *Mon. Wea. Rev.,* **129,** 2884–2903.

Burgers, G., P. J. V. Leeuwen, and G. Evensen, 1998: Analysis scheme in the ensemble Kalman filter. *Mon. Wea. Rev.,* **126,** 1719–1724.

Evensen, G., 1994: Sequential data assimilation with a nonlinear quasi-geostrophic model using Monte Carlo methods to forecast error statistics. *J. Geophys. Res.,* **99 (C5),** 10 143–10 162.

——, 2003: The ensemble Kalman filter: Theoretical formulation and practical implementation. *Ocean Dynamics,* **53,** 343–367.

Houtekamer, P. L., and H. L. Mitchell, 1998: Data assimilation using an ensemble Kalman filter technique. *Mon. Wea. Rev.,* **126,** 796–811.

——, 2001: A sequential ensemble Kalman filter for atmospheric data assimilation. *Mon. Wea. Rev.,* **129,** 123–137.

Lin, Y.-L., R. D. Farley, and H. D. Orville, 1983: Bulk parameterization of the snow field in a cloud model. *J. Climate Appl. Meteor.,* **22,** 1065–1092.

Richardson, Y. P., 1999: The influence of horizontal variations in vertical shear and low-level moisture on numerically simulated convective storms. Ph.D. dissertation, University of Oklahoma, 236 pp.

Smith, P. L., Jr., C. G. Myers, and H. D. Orville, 1975: Radar reflectivity factor calculations in numerical cloud models using bulk parameterization of precipitation processes. *J. Appl. Meteor.,* **14,** 1156–1165.

Tong, M., and M. Xue, 2005: Ensemble Kalman filter assimilation of Doppler radar data with a compressible nonhydrostatic model: OSS Experiments. *Mon. Wea. Rev.,* **133,** 1789–1807.

Weisman, M. L., and J. B. Klemp, 1982; the dependence of numerically simulated convective storms on vertical wind shear and buoyancy. *Mon. Wea. Rev.,* **110,** 504–520.

Whitaker, J. S., and T. M. Hamill, 2002: Ensemble data assimilation without perturbed observations. *Mon. Wea. Rev.,* **130,** 1913–1924.

Wood, V. T., and R. A. Brown, 1997: Effects of radar sampling on single-Doppler velocity signatures of mesocyclones and tornadoes. *Wea. Forecasting,* **12,** 928–938.

Xue, M., K. K. Droegemeier, and V. Wong, 2000: The Advanced Regional Prediction System (ARPS) - A multiscale nonhydrostatic atmospheric simulation and prediction tool. Part I: Model dynamics and verification. *Meteor. Atmos. Physics,* **75,** 161–193.

——, ——, ——, A. Shapiro, K. Brewster, F. Carr, D. Weber, Y. Liu, and D.-H. Wang, 2001: The Advanced Regional Prediction System (ARPS) - A multiscale nonhydrostatic atmospheric simulation and prediction tool. Part II: Model physics and applications. *Meteor. Atmos. Physics,* **76,** 143–165.

——, D.-H. Wang, J.-D. Gao, K. Brewster, and K. K. Droegemeier, 2003: The Advanced Regional Prediction System (ARPS), storm-scale numerical weather prediction and data assimilation. *Meteor. Atmos. Physics,* **82,** 139–170.

——, M. Tong, and K. K. Droegemeier, 2005a: An OSSE framework based on the ensemble square-root Kalman filter for evaluating the impact of data from radar networks on thunderstorm analysis and forecast. *J. Atmos. Oceanic Technol.,* submitted.

——, ——, and ——, 2005b: Impact of radar configuration and scan strategy on assimilation of radar data using ensemble Kalman filter. Preprints, *9th Symposium on Integrated Observing and Assimilation Systems for the Atmosphere, Oceans, and Land Surface,* San Diego, CA, Amer. Meteor. Soc., CD-ROM, 9.3.